Received: 28 February 2022 | Revised: 22 February 2022 | Accepted: 27 June 2022

IET Renewable Power Generation

DOI: 10.1049/rpg2.12550

ORIGINAL RESEARCH

All-DC offshore wind farms: When are they more cost-effective than AC designs?

Victor Timmers[1] | Agustí Egea-Àlvarez[1] | Aris Gkountaras[2] | Rui Li[1] | Lie Xu[1]

[1]Department of Electronic and Electrical Engineering, University of Strathclyde, Glasgow, UK

[2]Siemens Gamesa Renewable Energy, Hamburg, Germany

Correspondence
Victor Timmers, Department of Electronic and Electrical Engineering, University of Strathclyde, Glasgow, UK.
Email: victor.timmers@strath.ac.uk

Funding information
Siemens Gamesa Renewable Energy; Engineering and Physical Sciences Research Council, Grant/Award Number: EP/T517665/1

Abstract

The use of MVDC collector systems has been proposed as a way to reduce the levelised cost of energy (LCOE) of offshore wind farms. This study provides a quantitative assessment of the conditions required for such all-DC wind farms to be cost-effective. A comprehensive LCOE analysis of two AC and two all-DC wind farm designs is performed, with sensitivity studies on wind farm size, distance from shore, collector voltage, and component costs. The results show that for MVDC-based wind farms to be more cost-effective than equivalent HVDC wind farms, the DC/DC converter cost must be less than 90% of the cost of an equivalent MMC, with a cost reduction of 25% for the DC platform. Alternatively, if cost reductions of 30% can be achieved for the DC platform, then the DC/DC converter can be the same cost as an equivalent MMC. For all-MVDC wind farms without HVDC conversion stage to have the lowest LCOE, the collector voltage must be increased, preferably to ±100 kV or above. The all-MVDC configuration can also become cost-effective if a reduction of more than 50% in the cable installation cost can be achieved, for example, through the simultaneous burial of multiple cables.

1 | INTRODUCTION

The latest offshore wind farms under construction and in planning are the largest and furthest from shore ever. In the UK, preparation work has started for three 1200 MW Doggerbank offshore wind farms, located between 130 km and 190 km from shore [1], as well as for the 1400 MW Sofia offshore wind, located 220 km from shore [2]. At the same time, strike prices and subsidies for offshore wind have been decreasing at every auction [3, 4], which means the offshore wind industry must continually innovate to become more cost-effective.

One of the proposed methods in the literature to reduce the levelised cost of energy (LCOE) for offshore wind is by using MVDC cables in the wind farm collection network instead of conventional MVAC cables. Such all-DC wind farms have potential advantages, including a higher collector power density, cable cost reductions, and reductions in the weight and size of the offshore converters and associated platforms [5].

Previous research [6] has shown that the economic evaluations of all-DC wind farms in the literature vary significantly in their outcomes. This is due to differences in studied configurations, methodology, and uncertainties associated with immature technology such as high power, high step-up ratio DC/DC converters. In addition, the costs of offshore wind farm components can be difficult to determine, due to the sensitive nature of commercial data and the site-specific conditions that are unique to each wind farm.

In terms of studied configurations, a large range of designs has been proposed in the literature. These designs can be categorised into parallel and series topologies. In the parallel designs, the voltage is increased using DC/DC converters, located either on an offshore platform [7], inside the wind turbines [8], or both [9, 10]. In series designs, the voltage is instead increased through the series connection of all wind turbines in the wind farm [11] or the series connection of wind turbines in each string [12].

The methodologies used in cost-benefit analyses of all-DC wind farms in the literature is inconsistent, which further complicates the selection of the optimal configuration [6]. For example, some studies only investigate a single aspect of cost-effectiveness, such as capital cost [13], efficiency [14] or reliability [15], which can have a large impact on the study outcome.

In addition, most studies only investigate a single wind farm size and distance from shore, which makes their conclusions difficult to generalise. For example, a study by [7] investigated both costs and losses for several AC and DC configurations of a 1000 MW wind farm located 100 km from shore. They found that the DC parallel string collector was the most cost-effective. This is in contrast to [16], who also investigated both costs and losses of AC and DC configurations, but considered 100 MW and 300 MW wind farms. They found that the AC configuration was more cost-effective in both cases. This suggests that wind farm design parameters may impact the decision to use an AC or DC collector system.

A limited number of studies have performed sensitivity analyses to account for this uncertainty. In [17], a number of DC wind farm configurations were compared to an AC wind farm, with sensitivity studies on multiple component costs, distance from shore and wind turbine rating. They found that these factors impacted whether the DC configurations performed better than AC. However, this study did not draw any quantitative conclusions about the requirements for component costs.

1.1 | Contributions

This study aims to fill this gap by answering the question: what conditions are required for DC wind farms to be preferred over the traditional AC design? As part of this work, the following contributions are made that have not yet been published in other literature:

This study is the first to quantitatively define the conditions that are required for DC wind farms to be cost-effective by performing sensitivity studies on wind farm size, distance from shore, DC/DC converter cost, platform cost, cable cost and collector voltage. The results of this can be used as design targets when developing novel components for DC wind farms, such as the DC/DC converter.

The analysis includes the assessment of an all-MVDC wind farm topology, as well as a comparison to two traditional designs (all-AC and AC/HVDC). There are currently no cost estimates for this DC design and most studies only consider a comparison to a single AC wind farm topology.

The cost-benefit analysis of the AC and DC wind farms is the first which includes an assessment of multiple sources of data for wind farm cost components and their impact on the wind farm cost-effectiveness. Existing publications only consider a single source of data for their cost and rarely include any sensitivity analyses.

2 | CONFIGURATIONS

This study considers four configurations: two traditional designs with AC collectors and two novel designs using DC collectors. The selection of all-DC configurations was based on [6], which identified the standard parallel and dispersed parallel designs to be most promising in terms of economic performance. Series designs, despite having potential cost advantages, were found to have challenges with reliability [11], insulation [18], voltage balancing [19], and maintaining the transmission voltage [19]. This high technological risk means these series designs are unlikely candidates for commercialisation in the near future. These were therefore excluded from the analysis.

2.1 | All-AC

The first tested configuration is the all-AC wind farm, illustrated in Figure 1a. This is the traditional configuration where the wind turbines are parallel connected in strings using 66 kV AC cables. The strings connect to an offshore substation with two 50 Hz transformers to step up the voltage. This is then exported using 230 kV HVAC cables. Reactive compensation in the form of shunt reactors are often connected to offset the cable capacitance. These can be located at the onshore substation, offshore substation, or on a separate platform, depending on the total cable length.

2.2 | AC/HVDC

The AC/HVDC wind farm configuration is illustrated in Figure 1b. This design has an identical collector system to that of the all-AC configuration. The voltage is stepped up using one or more 50 Hz transformers and is then converted to HVDC by a modular multilevel converter (MMC). In the past, an offshore substation was typically used to house the step-up transformers before connecting to the HVDC platform, such as at the Dolwin cluster in Germany [20]. However, recent designs that use 66 kV cables remove the need for the offshore substation platform, instead housing all transformers on the HVDC platform [21]. This paper considers this second design. The power is exported from the HVDC platform to shore using HVDC cables rated at ±320 kV. Finally, a second MMC is located at the onshore substation before connecting to the network.

2.3 | MVDC/HVDC

The MVDC/HVDC configuration is shown in Figure 2a. This configuration uses an MVDC collector system, typically rated at ±40 kV. The wind turbines use an isolated DC/DC converter with medium frequency transformer (MFT) after the rectification stage to boost the voltage to this level. A large range of DC/DC converters have been proposed in the literature [22]. This study assumes the converter topology consists of a cascaded single-active bridge (SAB) with phase shift [23]. The offshore substation uses a high power version of this DC/DC converter. The DC/DC converter is smaller than the traditional MMC converter, resulting in a reduction in the HVDC platform footprint. An MMC converts the voltage back to AC at the onshore substation.

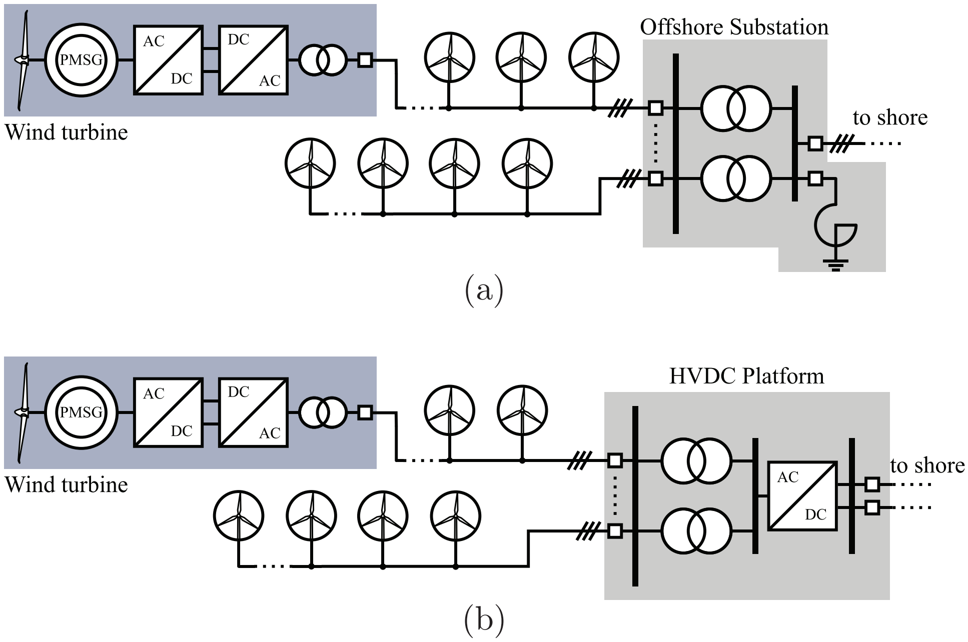

FIGURE 1 Single line diagrams of the investigated AC wind farm configurations: (a) all-AC, (b) AC/HVDC

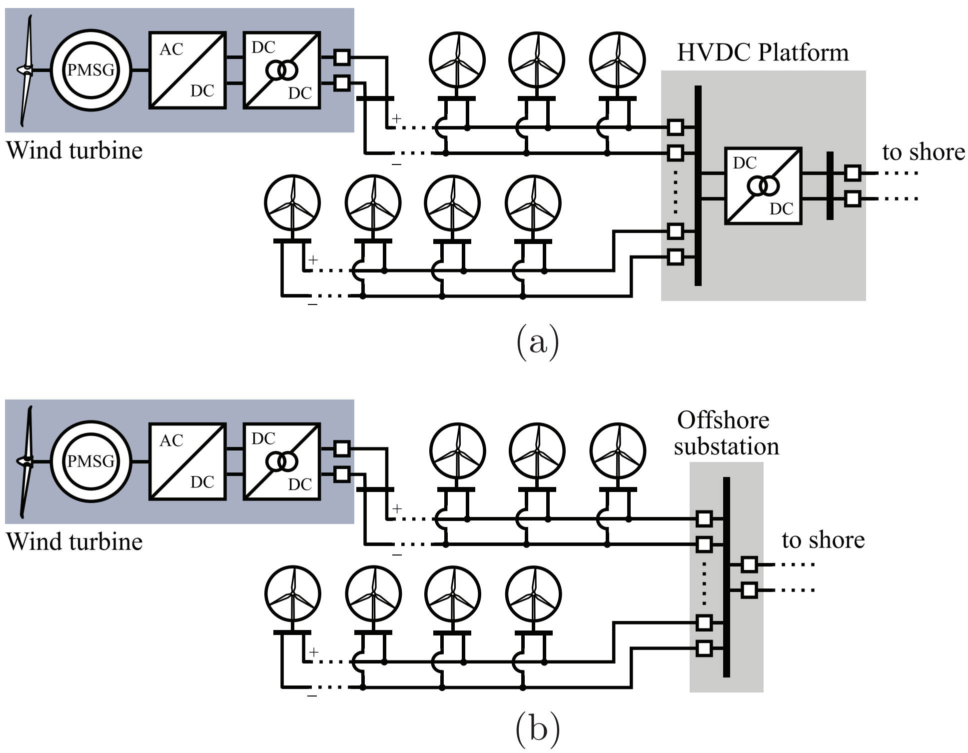

FIGURE 2 Single line diagrams of the investigated DC wind farm configurations: (a) MVDC/HVDC, (b) all-MVDC

2.4 | All-MVDC

The final configuration is the all-MVDC wind farm, as shown in Figure 2b. This design uses the same ±40 kV MVDC collector system as the previous design. This configuration however, does not have a central high power DC/DC converter on the offshore platform to step up the voltage. Instead, the offshore platform is much smaller and only consists of DC connection protection equipment. The export cables to shore have the same voltage as the collector system. Here too, an MMC

TABLE 1 Wind farm design results for the base case

Parameter	all-AC	AC/HVDC	MVDC/HVDC	all-MVDC
Wind turbine rating (MW)	15	15	15	15
Number of strings	14	14	12	12
Wind turbines per string	5	5	6	6
String cable CSAs (mm^2)	95, 95, 185, 300, 630	95, 95, 185, 300, 630	95, 120, 240, 400, 630, 800	95, 120, 240, 400, 630, 800
Number of transformers	4	4	0	0
Transformer MVA	265	265	–	–
Number of export cables	3	1	1	6
Export cable CSA (mm^2)	1200	1400	1400	2400
Reactive compensation (MVAr)	950	0	0	0

is located at the onshore substation before connecting to the grid.

2.5 | Design

The study considers wind farms ranging in size from 200 MW to 1500 MW, with a base case of 1000 MW. As a result, a generic design procedure was used to determine the wind farm parameters. The results for the base case design of each of the four configurations are shown in Table 1.

The collector system is considered to be a standard rectangular arrangement of the wind turbines, with an inter-turbine spacing of 7 rotor diameters [7] or 1.5 km. The number of wind turbines per string is limited by the maximum collector cable cross-sectional area (CSA), which is 800 mm^2 [24]. The wind turbines were distributed evenly to all strings. The CSA of all collector cables are then calculated based on the maximum current each is expected to conduct, resulting in smaller CSA for the first turbines in a string. The available AC and DC cable sizes and ratings were obtained from publicly available datasheets [25, 26].

For the AC designs, the number of MV busbars is calculated assuming a maximum continuous current rating of 2.5 kA per busbar [27, 28]. Each busbar has a step-up transformer connected with a rating taking into account a minimum power factor of 0.95, based on the grid code [29]. The MV busbars are connected together using normally open bus ties, which can reconfigure the power flow in case of transformer failure [28]. The maximum number of transformers per substation is assumed to be four due to the constructional constraints [27]. If more transformers are required, additional AC substations will be needed to accommodate these.

The maximum HVAC and HVDC cable CSAs were set to be 2000 mm^2 and 3000 mm^2, respectively. Cable sizes, ratings, and AC capacitance were obtained or extrapolated from [25, 26]. For the all-AC configuration, the capacitance is considered to be fully compensated using reactive compensation equipment. The distribution of reactive compensation is based on [30, 31].

3 | COST CALCULATION

The aim of the cost calculation is to provide an estimate of the capital expenditure (CAPEX) for the investigated configurations. Offshore wind farms consist of a huge number of components. In the CAPEX estimation, only the most significant cost contributors are included. These consist of the wind turbines including drivetrain and foundation, the collector cables, the offshore substation including transformers and switchgear, the high power converters, the export cables and the onshore substation. For the all-AC wind farm, reactive compensation is required and the costs associated with shunt reactors and any additional platforms are also included.

Since cost information is provided in different currencies and available for various years, it is necessary to normalise all cost data. A base currency of M€$_{2021}$ was selected for this. The currency conversions are performed using the average exchange rate of the source year, obtained from [32]. Costs are then adjusted to the 2021 value of the euro based on the historical inflation rate, obtained from [33].

3.1 | Wind turbine

The cost of AC wind turbines has been estimated by a number of sources [24, 34, 35] and is calculated based on the wind turbine rated power. The cost, including acquisition, foundation, transport and installation, is shown in Figure 3a. The median cost estimate by [34] is given in (A.1) in the appendix.

There is currently no cost data available for wind turbines that use DC electrical drivetrains as no commercial designs have been implemented. Most cost estimates in the literature therefore consider the cost of DC wind turbines to be a factor of the AC wind turbine cost [17]. The BVG Associates report [24] estimates the power take-off and control system to cost approximately 6.6% of the overall turbine cost, including the foundation and installation. For this cost-benefit analysis, the DC/DC converter with MFT is assumed to have a cost that is 50% higher than the conventional back-to-back converter due

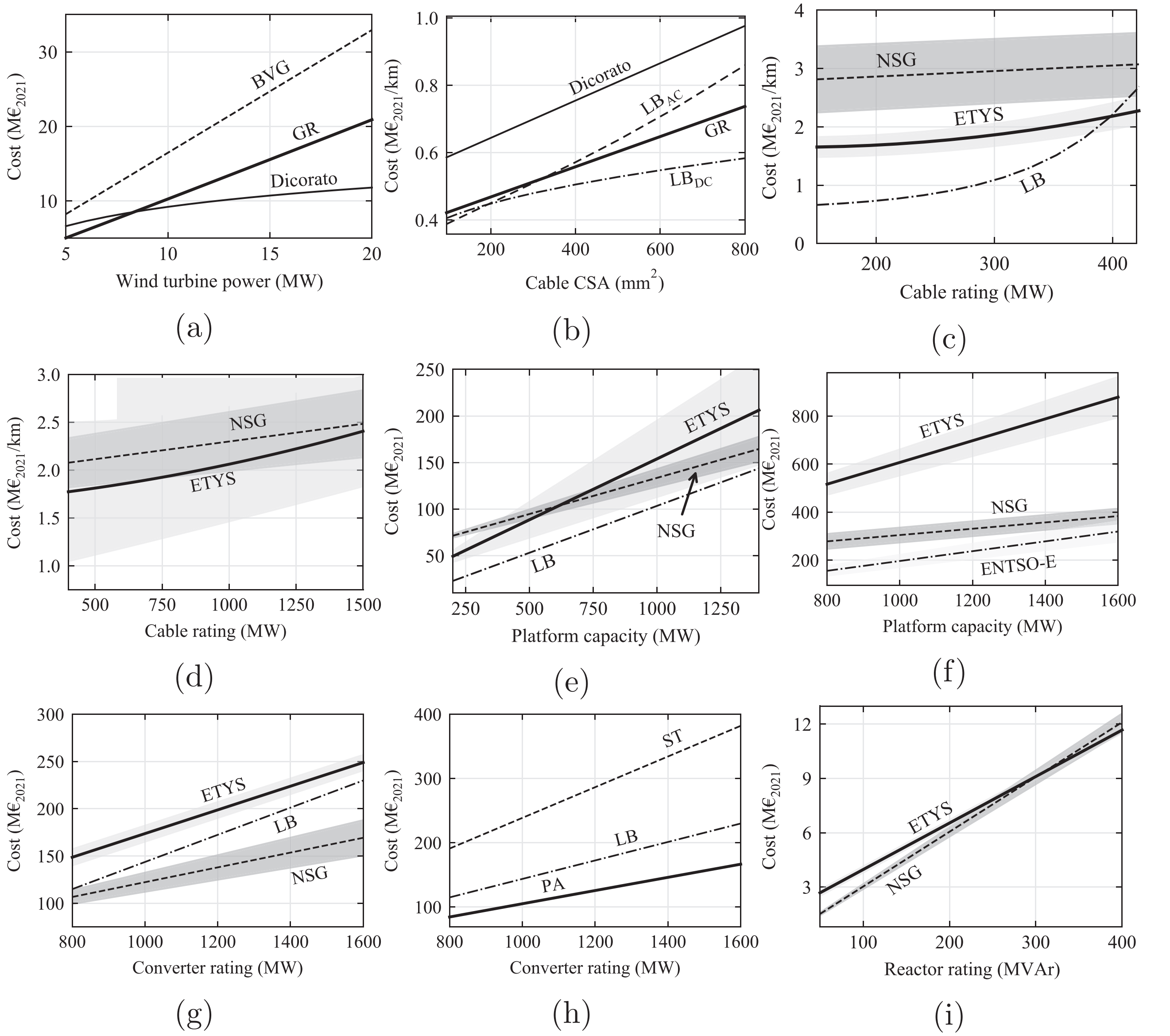

FIGURE 3 Wind farm component costs, calculated using various sources including Dicorato et al. [35], Gonzalez-Rodriguez et al. (GR) [34], BVG associates (BVG) [24], Lundberg (LB) [12], NorthSeaGrid (NSG) [36], UK Electricity Ten Year Statement (ETYS) [37], European Network of Transmission System Operators for Electricity (ENTSO-E) [38], Parker and Anaya-Lara (PA) [7], Stamatiou (ST) [39] : (a) wind turbine, (b) MVAC and MVDC cables (c) HVAC cables, (d) HVDC cables, (e) AC platform, (f) DC platform, (g) AC/DC converter, (h) DC/DC converter, (i) shunt reactor

to the additional conversion stage. The total DC wind turbine cost is therefore 3.3% higher compared to AC.

3.2 | Collector cables

Most current offshore wind farm projects use radial AC collection systems with voltages of 33 kV. More recent offshore wind farms are planned to have voltages of 66 kV. There is also ongoing research and industrial interest in increasing this voltage to 132 kV for future wind farms. Cost estimates for medium voltage cables are provided in [12, 34, 35] and are shown in Figure 3b. The median estimate for AC cables is [12] for most cable sizes. This is calculated using (A.2).

Cost estimates for DC collector cables are more difficult to obtain as medium voltage DC submarine cables are not yet widely used. One cost estimate is provided [12]. This has also been used in many other publications [7, 17, 39]. The equation (A.3) for this is given in the appendix.

3.3 | Export cables

Cost estimates for HVAC cables found in the literature [12, 36, 37] are shown in Figure 3c. The same sources also provide estimates for HVDC cables, shown in Figure 3d. The median cost for most cable sizes is given by [37]. The equation (A.4) is provided in the appendix.

3.4 | Platforms

The AC platform cost is provided by various sources [12, 36, 37], and is shown in Figure 3e. The median estimate provided by [36] is calculated using Equation (A.5). The all-MVDC configuration uses a small protection platform which is assumed to be half the cost of the AC platform. Similarly, the DC platform cost is estimated by [36–38], as shown in Figure 3f. The median cost provided by [36] is calculated using Equation (A.6). The MVDC/HVDC configuration uses a smaller and lighter DC/DC converter compared to the conventional HVDC converters used in the AC/HVDC design. The cost of this platform was assumed to be 75% of the DC platform cost in the base case.

3.5 | Converters

The cost of the high power AC/DC converter used in the AC/HVDC configuration is provided by [12, 36, 37], and shown in Figure 3g. The cost for a DC/DC converter is more difficult to obtain since no commercial designs have been applied to wind farms so far. Estimates have been made by [7, 12, 39], which can be observed in Figure 3h. The median for both converter types is provided by [12] and calculated using Equation (A.7).

3.6 | Equipment

Other equipment which contributes to the cost to a lesser extent include the transformers, switchgear and shunt reactors. The transformer costs can be approximated using Equation (A.8), provided by Dicorato [35]. The cost of the offshore GIS switchgear is provided in the 2015 ETYS [37] using Equation (A.9). The cost of DC switchgear used in the DC wind farm configurations was assumed to be twice the cost of AC switchgear, based on [39]. The shunt reactor costs are given by [36, 40] and are shown in Figure 3i. These can be approximated using Equation (A.10). If the shunt reactor is located on the offshore platform, the cost of the additional weight is provided by [41] and calculated using (A.11). If the shunt reactor requires a separate offshore platform at the cable midpoint, this is calculated using (A.5).

3.7 | Operational costs

The annual operational expenditure (OPEX) of each component was estimated as a proportion of the CAPEX, based on median values suggested in [36]. These are given in Table 2. The net present value (NPV) of the OPEX is calculated by discounting the annual OPEX over the lifetime of the wind farm, using the equation

$$\mathrm{OPEX_{NPV}} = \frac{\sum_{n=1}^{N} O_n}{d} \cdot \left(1 - \frac{1}{(1+d)^{L_T}}\right), \tag{1}$$

TABLE 2 Component annual operational expenditures, with CAPEX as base [36]

Component	OPEX (pu)
Cables	0.025
Platform	0.02
Onshore converter	0.007
Offshore converter	0.02
Switchgear	0.007
Transformer	0.0015
Shunt reactor	0.0015

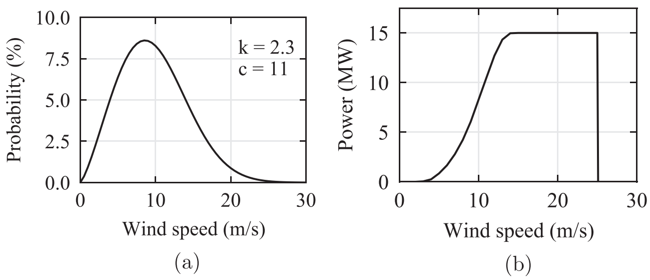

FIGURE 4 Wind turbine power calculation inputs: (a) Weibull probability distribution of the wind speed, (b) wind turbine power curve

where $\mathrm{OPEX_{NPV}}$ is the net present value of the operational costs in M€ $_{2021}$, O_n is the annual OPEX of component n, d is the discount rate, and L_T is the lifetime in years. The base case considers a discount rate of 6% and a lifetime of 27 years [24].

4 | LOSSES, RELIABILITY AND LCOE CALCULATION

4.1 | Losses

The energy losses of each component are dependent on the power output of the wind turbines. A Weibull probability distribution of the wind speed was assumed, resulting in the following expression

$$T(v) = 8760 \cdot \frac{k}{c}\left(\frac{v}{c}\right)^{k-1} \cdot \exp\left[-\left(\frac{v}{c}\right)^{k}\right], \tag{2}$$

where $T(v)$ is the annual hours with wind speed v, c is the scale parameter, and k is the shape parameter. A typical value of 2.3 for k and 11 for c was selected, resulting in the distribution illustrated in Figure 4a. The power output of the wind turbines at each wind speed is calculated using a generic power curve, scaled to the wind turbine rating. This is shown in Figure 4b. A typical reduction of 8.5% in the wind speed is included to take into account the effect of wakes in the wind farm.

TABLE 3 Component no-load and full-load losses

Component	Source	NLL (%)	FLL (%)
WT converter	[42]	0.2	2.0
MMC converter	[43]	0.1	0.8
Transformer	[44]	0.055	0.3

The losses for each cable run were calculated using the equation

$$L_{cab} = \sum_{v=v_{min}}^{v_{max}} T(v) \cdot 3\big(I_{cab}(v)\big)^2 R_{cab}, \quad (3)$$

where $T(v)$ is the annual hours with wind speed v, $I_{cab}(v)$ is the current passing through the cable at wind speed v, and R_{cab} is the cable resistance. For DC cables, the factor 3 is replaced by a factor 2 due to the reduction in conductors per cable.

The losses of the wind turbine converter, transformer, AC/DC converter and shunt reactor were calculated using the equation

$$L_n = \sum_{v=v_{min}}^{v_{max}} T(v) \cdot \left(NLL + \left(\frac{P_n(v)}{P_{max}} \right)^2 \cdot FLL \right), \quad (4)$$

where L_n are the losses in per unit of component n, $P_n(v)$ is the power at wind speed v, P_{max} is the component rated power, NLL and FLL are the component no-load and full-load losses in per unit, respectively. These are provided in Table 3. The shunt reactors are assumed to have identical losses to the transformers.

The losses of DC/DC converters with various topologies were estimated in [23]. The base case assumes a single-active bridge topology with phase shift operation, which has losses ranging from 2.75% at low loading to 1.4% losses at full load [23].

4.2 | Reliability

The reliability of each configuration was taken into account by calculating the expected energy not supplied (EENS) due to repairs of each component, based on the approach in [45]. The unavailability due to the failure of a component n is expressed using

$$U_n = \sum_{v=v_{min}}^{v_{max}} T(v) \cdot F_n(v) \cdot \lambda_n \cdot r_n \quad (5)$$

where $T(v)$ is the annual hours with wind speed v, λ_n is the failure rate of component n, r_n is the repair time, and $F_n(v)$ is the proportion of the wind farm out of service due to the failure of the component. The failure rates and repair times used in the calculation are set out in Table 4.

TABLE 4 Component failure rates and repair times

Component	Source	λ (yr^{-1})	r (hrs)
AC cable	[46]	0.0007/km	1440
DC cable	[46]	0.0004/km	2304
AC circuit breaker	[47]	0.024	720
Transformer	[48]	0.025	3000
WT converter	[49]	0.15	720
MMC converter	[50]	0.0153	1664

Failure rate and repair time data varies significantly between sources. In [48], the failure rate of offshore converters is found to be 1 failure per year with a repair time of up to 168 h, whereas the failure rate and repair time used in [50] differ by an order of magnitude: 0.0153 failures/year and 1664 h, respectively. This difference is due to the types of failures considered, as well as the consideration of travel time.

For offshore wind farms, the transportation of technicians and equipment has a major impact on overall repair time, especially since this is impacted by adverse weather conditions [51]. The downtime of the wind turbine converter and circuit breakers were therefore assumed to be 30 days, despite their much lower onshore repair times.

The reliability of the DC technology such as the DC/DC converter and DC circuit breakers is not known and will be dependent on the topology used. For this study, the unavailability of the DC/DC converter was assumed to be twice that of the AC/DC converter plus the unavailability of the transformer. The failure rate of DC circuit breakers was assumed to be twice that of AC circuit breakers [39].

For the calculation of $F_n(v)$, it was assumed that any failure of the collector cables or string circuit breaker would result in the disconnection of the entire string. For transformer failures, the wind farm was assumed to be reconfigured to divert the energy to the remaining transformers, curtailing the wind turbine output to prevent exceeding the transformer ratings if necessary. Similarly, if one of the export cables fails, the energy is assumed to be diverted to any remaining healthy cables up to their maximum rated capability.

4.3 | Levelised cost of energy

The levelised cost of energy was used to compare the economic performance of the four configurations. This is calculated using the equation

$$LCOE = \frac{C_{total} + OPEX_{NPV}}{(1 - L_{total} - U_{total}) \cdot AEP_{NPV}}, \quad (6)$$

where C_{total} is the total CAPEX, $OPEX_{NPV}$ is the net present value of the OPEX, L_{total} are the total losses in per unit, U_{total} is the total unavailability in per unit, and AEP_{NPV} is the discounted gross annual energy production.

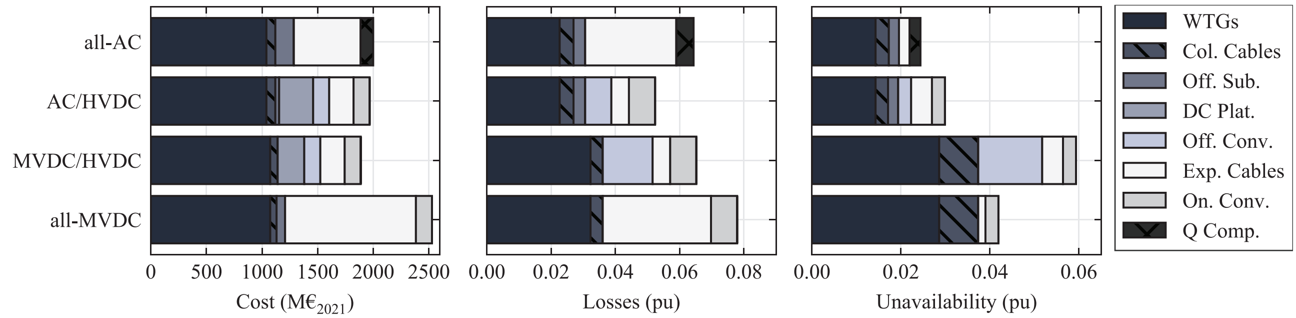

FIGURE 5 Costs, losses, and unavailability of each component for the considered configurations in the base case

5 | RESULTS

5.1 | Base case

The base case considers a 1000 MW wind farm at a distance of 100 km from shore. The cost, losses, and reliability breakdown for each of the four configurations is shown in Figure 5. The cost results show that the MVDC/HVDC configuration has the lowest overall cost, mainly due to the lower DC platform and cable costs. The all-AC and AC/HVDC configurations have similar capital costs. The latter has a reduction in cable costs but these are largely offset by the converter and DC platform costs. The all-MVDC configuration does not provide significant cost savings in this case despite having the lowest platform cost of all configurations. This is because it requires a large number of export cable circuits due to the low export voltage. This significantly increases the cable costs.

In terms of efficiency, the AC/HVDC and MVDC/HVDC configurations provide improvements over the all-AC configuration due to the reduction in export cable losses. The MVDC/HVDC configuration, however, suffers from high converter losses in the base case, resulting in more limited efficiency improvements. The all-MVDC configuration has increased overall losses due to the lower export voltage, despite having no converter or transformer losses on its offshore substation.

The unavailability figure shows that the all-AC configuration has the highest reliability due to the mature technology used and absence of converters. Conversely, the MVDC/HVDC and all-MVDC configurations have the lowest reliability due to the relatively high assumed failure rate of the DC/DC converter and DC switchgear.

5.2 | Optimal configuration

The calculated LCOE for the base case shows that the MVDC/HVDC configuration is the preferred option with an LCOE of 47 € $_{2021}$/MWh. The calculated LCOE for other distances are shown in Figure 6. The figure shows that for a 1000 MW wind farm, the all-AC configuration has the lowest LCOE up to 80 km. The AC/HVDC and MVDC/HVDC configurations have near identical LCOEs and are most cost-effective beyond 80 km. The all-MVDC option is more expensive for all distances.

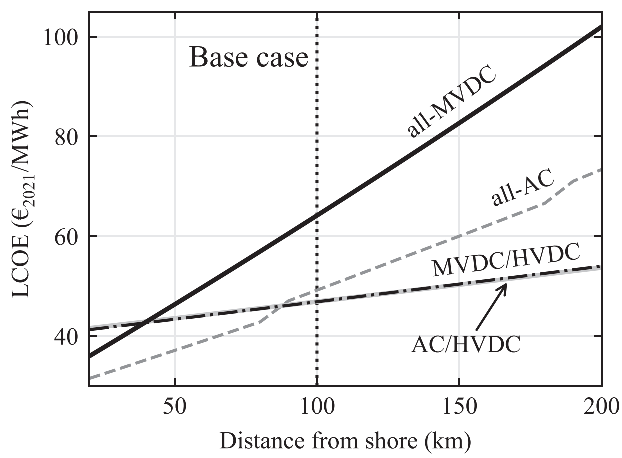

FIGURE 6 Levelised cost of energy by distance from shore for a 1000 MW wind farm using the considered configurations

It can be seen from the figure that as the distance to shore increases, the LCOE of the configurations increases linearly due to a rise in export cable costs and losses. The all-AC option has additional step increases at 90 km and 190 km because at these distances additional platforms are required to house the reactive compensation equipment along the cable circuit.

The optimal configuration was calculated for each combination of wind farm size ranging from 200 MW to 1500 MW and distance from shore between 20 km and 200 km. The base case considers a collector voltage of 66 kV AC or ±40 kV DC. The result of this calculation is shown in Figure 7. The results show that the traditional all-AC configuration is the most cost-effective for wind farms of any size up to approximately 80 km from shore, or small wind farms of up to 500 MW at any distance from shore. The MVDC/HVDC option has the lowest LCOE in two regions: large wind farms of more than 800 MW at medium distances of 80 km to 140 km, and medium wind farm sizes of 400 MW to 600 MW at long distances of more than 120 km. For large wind farms at far distances, the AC/HVDC option becomes more cost-effective. The all-MVDC option does not have the lowest LCOE at any point in the base case.

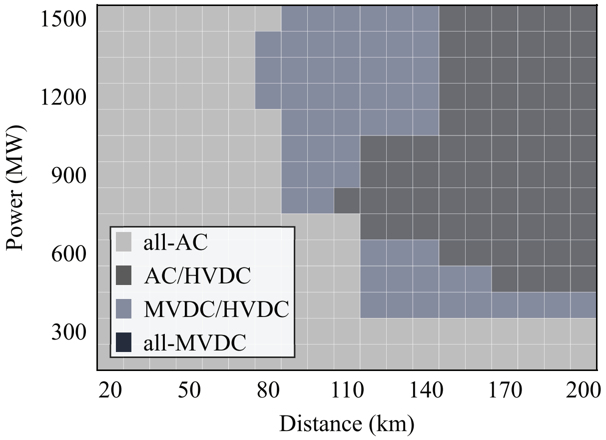

FIGURE 7 Optimal configuration in the base case for varying wind farm size and distance from shore

6 | SENSITIVITY STUDIES

A series of sensitivity studies were performed to take into account the uncertainties of the most important elements for both all-DC configurations including the cost and performance of the DC/DC converter, the DC platform costs, the collector voltage and the export cable installation costs.

6.1 | DC/DC converter

A sensitivity study was performed to take into account the uncertainty of the DC/DC converter technology. The cost, losses and failure rate of the DC/DC converter were varied as a proportion of the base case values. The results of this sensitivity analysis are shown in Figure 8a.

The figure shows the DC/DC converter cost and performance have a large impact on the cost-effectiveness of the MVDC/HVDC configuration. The maximum DC/DC converter allowable cost, losses, and failure rate are 1.05 pu of the base case values. At this point, the MVDC/HVDC configuration has the lowest LCOE under very limited conditions: 400 MW wind farms located between 120 km and 190 km from shore.

As the cost and performance improve, the MVDC/HVDC option becomes the optimal configuration for more wind farms. The largest improvement can be seen at 0.9 pu, at which point the MVDC/HVDC configuration is preferred over the AC/HVDC option for all wind farm sizes and distances from shore. Further cost reductions and performance improvements have a smaller impact, marginally reducing the distance from shore at which the MVDC/HVDC configuration becomes the most cost-effective option.

6.2 | DC platform cost

The main advantage of the MVDC/HVDC configuration over the AC/HVDC configuration is its DC platform cost reduction. The precise cost savings will be dependent on the weight and space requirements of the DC/DC converter and the DC platform design. A sensitivity study was performed to determine the cost reduction requirements. The results of this analysis are shown in Figure 8b.

The figure shows that the MVDC platform must provide a minimum of 20% cost savings for the MVDC/HVDC option to be the optimal configuration under limited conditions. A significant improvement can be seen when the MVDC platform is 27.5% cheaper than an equivalent HVDC platform. For the MVDC/HVDC configuration to be more cost-effective than the AC/HVDC configuration for all wind farm sizes and distances from shore, a cost reduction in the DC platform of 30% is required.

6.3 | Collector voltage

The all-MVDC configuration is highly dependent on the selected collector voltage. Increasing the voltage will reduce the number of cable circuits required in the all-MVDC export system, which is the main source of capital costs for this configuration. A sensitivity study was performed varying the collector voltage up to ±140 kV DC. Note that higher collector voltages result in additional challenges in terms of insulation requirements and wind turbine converter capability, which have not been taken into account here. The results for this study are shown in Figure 9a.

The figure shows that a minimum voltage of ±60 kV is required for the all-MVDC option to have the lowest LCOE for 200 MW wind farms at distances of more than 110 km from shore. Further increases in the voltage show the all-MVDC option becomes increasingly cost-effective for larger wind farms at medium distances. At a collector voltage of ±100 kV, the all-MVDC option is the most cost-effective for wind farms up to 900 MW at distances between 90 km and 120 km. If the collector voltage can be increased to ±140 kV, the all-MVDC option has the lowest LCOE for the majority of wind farm sizes and distances.

6.4 | Cable installation cost

The all-MVDC configuration requires a large number of export cables, therefore any reduction in the cable installation cost will disproportionately benefit this configuration. A sensitivity study was performed on the cable installation cost, with the results shown in Figure 9b.

The figure shows that if the cable installation cost can be reduced by 50% or more, the all-MVDC option becomes cost-effective for small wind farms at large distances from shore, even when using ±40 kV cable circuits. Most of the installation cost is due to the hiring of vessels [24]. Therefore to achieve such a significant cost reduction, specialised equipment that can install several cables at once would likely be required.

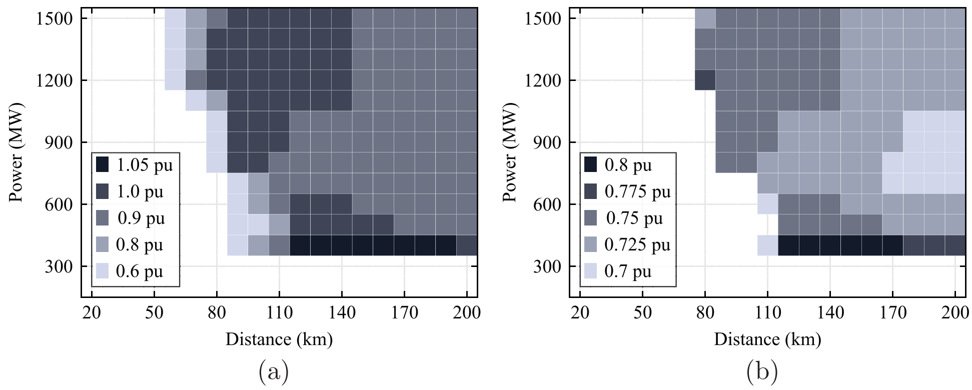

FIGURE 8 Wind farm size and distance from shore where the MVDC/HVDC configuration has the lowest LCOE, based on (a) converter cost, losses and failure rate compared to the base case, and (b) relative cost of MVDC platform compared to the HVDC platform

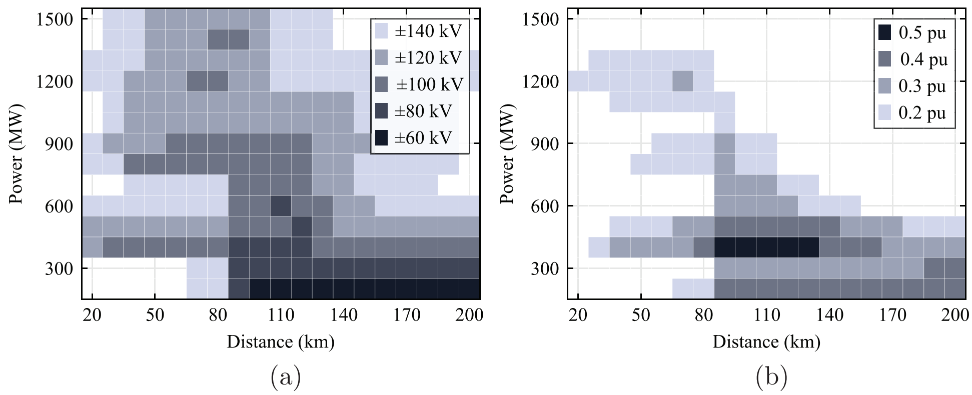

FIGURE 9 Wind farm size and distance from shore where the all-MVDC configuration has the lowest LCOE, based on (a) collector voltage, (b) export cable installation cost compared to the base case

7 | CONCLUSION

This paper investigated the conditions required for all-DC wind farms to be more cost-effective than existing AC configurations. A total of four wind farm configurations were assessed, including the all-AC, AC/HVDC, MVDC/HVDC, and all-MVDC designs. The analysis took into account the costs, losses, and reliability to calculate the wind farm LCOE. The optimal configuration with the lowest LCOE was calculated for wind farms ranging in size from 200 MW to 1500 MW at a distance from shore between 20 km and 200 km.

The results showed that for the base case, the all-AC option is preferred for wind farms of any size at distances up to 80 km from shore. The AC/HVDC option is optimal for large wind farms at very long distances of more than 150 km from shore. The MVDC/HVDC option has a very similar LCOE to the AC/HVDC option and is most cost-effective at the transition between all-AC and AC/HVDC. The all-MVDC option was found to always be more expensive than the other configurations in the base case.

The sensitivity studies showed that the main factors affecting the MVDC/HVDC cost-effectiveness were the costs of the DC/DC converter and DC platform. For the MVDC/HVDC to be more cost-effective than equivalent AC/HVDC wind farms at any size and distance, the DC/DC converter cost must be less than 90% of the cost of an equivalent MMC, with a cost reduction of 25% for the DC platform. Alternatively, if the DC platform of the MVDC/HVDC configuration costs 30% less than that of the AC/HVDC option, then the DC/DC converter can be the same cost as an equivalent MMC.

The main factors affecting the all-MVDC option are the collector voltage and cable installation costs. A collector voltage of ±100 kV or more results in the all-MVDC option being preferred for small and medium wind farms at distances above 80 km from shore. If collector voltages of ±140 kV can be achieved, the all-MVDC option becomes the optimal configuration for most wind farm sizes and distances from shore. Alternatively, a reduction in cable installation costs of 50% or more is required for the all-MVDC option to be the most cost-effective configuration for small wind farms at long distances from shore.

Potential future work can include refining the cost-benefit analysis once DC/DC converter development is nearer commercialisation and performing case-studies for specific wind farm locations.

ACKNOWLEDGEMENTS

This work was funded by EPSRC Industrial CASE number EP/T517665/1 and Siemens Gamesa Renewable Energy.

CONFLICT OF INTEREST

The authors have declared no conflict of interest.

DATA AVAILABILITY STATEMENT

The data that support the findings of this study are available from the corresponding author upon reasonable request.

ORCID

Victor Timmers https://orcid.org/0000-0002-3775-6544

REFERENCES

1. Doggerbank wind farm - about the project. doggerbank.com/about/
2. Sofia offshore wind farm - project. sofiawindfarm.com/project/
3. Edwardes-Evans, H.: UK's fourth CfD renewable energy auction in late 2021 to aim for 12 GW. www.spglobal.com/platts/en/market-insights/latest-news/electric-power/112420-uks-fourth-cfd-renewable-energy-auction-in-late-2021-to-aim-for-12-gw
4. Durakovic, A.: Germany sets offshore wind targets, tweaks tendering procedure. www.offshorewind.biz/2020/11/06/germany-sets-offshore-wind-targets-tweaks-tendering-procedure/
5. Abeynayake, G., Li, G., Liang, J., Cutululis, N.A.: A review on mvdc collection systems for high-power offshore wind farms. In: 2019 14th Conference on Industrial and Information Systems (ICIIS), pp. 407–412. IEEE, Piscataway (2019)
6. Timmers, V., Egea Àlvarez, A., Gkountaras, A.: A systematic review of DC wind farm collector cost-effectiveness. In: 17th International Conference on AC and DC Power Transmission, pp. 114–119. IET, Stevenage (2021)
7. Parker, M.A., Anaya-Lara, O.: Cost and losses associated with offshore wind farm collection networks which centralise the turbine power electronic converters. IET Renew. Power Gener. 7(4), 390–400 (2013)
8. Lundberg, S.: Evaluation of wind farm layouts. EPE J. 16(1), 14–21 (2006)
9. Meyer, C., Hoing, M., Peterson, A., De Doncker, R.W.: Control and design of dc grids for offshore wind farms. IEEE Trans. Ind. Appl. 43(6), 1475–1482 (2007)
10. Max, L., Lundberg, S.: System efficiency of a dc/dc converter-based wind farm. Wind Energy: Int. J. Prog. Appl. Wind Power Conver. Technol. 11(1), 109–120 (2008)
11. Holtsmark, N., Bahirat, H.J., Molinas, M., Mork, B.A., Hoidalen, H.K.: An all-dc offshore wind farm with series-connected turbines: An alternative to the classical parallel ac model? IEEE Trans. Ind. Electron. 60(6), 2420–2428 (2012)
12. Lundberg, S.: Performance Comparison of Wind Park Configurations. Chalmers University of Technology, Göteborg, Sweden (2003)
13. Pan, J., Bala, S., Callavik, M., Sandeberg, P.: Platformless dc collection and transmission for offshore wind. In: 11th IET International Conference on AC and DC Power Transmission, pp. 1–6. IET, Stevenage (2015)
14. Tang, W., Shi, M., Li, Z., Yu, N.: Loss comparison study of mmc-hvdc and all-dc offshore wind farm. In: 2019 IEEE Innovative Smart Grid Technologies-Asia (ISGT Asia), pp. 171–175. IEEE, Piscataway (2019)
15. Bahirat, H.J., Kjølle, G.H., Mork, B.A., Høidalen, H.K.: Reliability assessment of dc wind farms. In: 2012 IEEE Power and Energy Society General Meeting, pp. 1–7. IEEE, Piscataway (2012)
16. Kucuksari, S., Erdogan, N., Cali, U.: Impact of electrical topology, capacity factor and line length on economic performance of offshore wind investments. Energies 12(16), 3191 (2019)
17. De Prada Gil, M., Domínguez García, J.L., Díaz González, F., Aragüés Peñalba, M., Gomis Bellmunt, O.: Feasibility analysis of offshore wind power plants with dc collection grid. Renew. Energy 78, 467–477 (2015)
18. Bahirat, H.J., Mork, B.A., Høidalen, H.K.: Comparison of wind farm topologies for offshore applications. In: 2012 IEEE Power and Energy Society General Meeting, pp. 1–8. IEEE, Piscataway (2012)
19. Zhang, H., Gruson, F., Rodriguez, D.M.F., Saudemont, C.: Overvoltage limitation method of an offshore wind farm with dc series-parallel collection grid. IEEE Trans. Sustain. Energy 10(1), 204–213 (2018)
20. GE Grid Solutions.: DolWin3 HVDC voltage source converters for efficient connection of renewable energy. www.gegridsolutions.com/products/applications/hvdc/hvdc-vsc-dolwin3-case-study-en-2018-11-grid-pea-0578.pdf
21. Skopljak, N.: TenneT's oss-less connection for Ørsted and EnBW german projects. www.offshorewind.biz/2019/09/06/tennets-oss-less-connection-for-orsted-and-enbw-german-projects/
22. Zhou, Y., Macpherson, D., Blewitt, W., Jovcic, D.: Comparison of dc-dc converter topologies for offshore wind-farm application. In: 6th IET International Conference on Power Electronics, Machines and Drives (PEMD 2012), pp. 1–6. IET, Stevenage (2012)
23. Dincan, C.: High Power Medium Voltage DC/DC Converter Technology for DC Wind Turbines. Aalborg University, (2018)
24. BVG Associates.: Guide to an offshore wind farm. The Crown Estate (2019). bvgassociates.com/wp-content/uploads/2019/04/BVGA-Guide-to-an-offshore-wind-farm-r2.pdf
25. ABB: Xlpe Submarine Cable Systems: Attachment to xlpe Land Cable Systems - User's Guide. ABB (2010)
26. ABB.: Hvdc light® Cables Submarine and Land Power Cables. ABB (2006)
27. DNV GL Energy.: 66 kV Systems for Offshore Wind Farms. TenneT (2015)
28. Krieg, T., Finn, J.: CIGRE Green Book - Substations. CIGRE, Paris (2021)
29. National Grid ESO.: The Grid Code - Issue 6. National Grid Electricity System Operator Limited, Warwick (2021)
30. Dakic, J., Cheah Mane, M., Gomis Bellmunt, O., Araujo, E.P.: Hvac transmission system for offshore wind power plants including mid-cable reactive power compensation: Optimal design and comparison to vsc-hvdc transmission. IEEE Trans. Power Delivery (2020)
31. Lauria, S., Schembari, M., Palone, F., Maccioni, M.: Very long distance connection of gigawatt-size offshore wind farms: extra high-voltage ac versus high-voltage dc cost comparison. IET Renew. Power Gener. 10(5), 713–720 (2016)
32. OFX.: Historical exchange rates (2021). Available from: www.ofx.com/en-gb/forex-news/historical-exchange-rates/
33. InflationTool.: Inflation calculator - euro (2021). www.inflationtool.com/euro
34. Gonzalez Rodriguez, A.G.: Review of offshore wind farm cost components. Energy Sustain. Develop. 37, 10–19 (2017)
35. Dicorato, M., Forte, G., Pisani, M., Trovato, M.: Guidelines for assessment of investment cost for offshore wind generation. Renew. Energy 36(8), 2043–2051 (2011)
36. Flament, A., Joseph, P., Gerdes, G., Rehfeldt, L., Behrens, A., Dimitrova, A., et al.: NorthSeaGrid - Annexes to the Final Report. 3E, DWG, DNG GL, ECN, CEPS, Imperial College (2014)
37. National Grid plc.: Electricity Ten Year Statement 2015: Appendix E - Technology. National Grid (2015)
38. European Network of Transmission System Operators for Electricity (ENTSO-E): Offshore transmission technology (2011). eepublicdownloads.entsoe.eu/clean-documents/pre2015/publications/entsoe/SDC/European_offshore_grid_-_Offshore_Technology_-_FINALversion.pdf
39. Stamatiou, G.: Techno-Economical Analysis of DC Collection Grid for Offshore Wind Parks. University of Nottingham (2010)
40. National Grid plc.: Electricity Ten Year Statement 2013: Appendix E - Technology. National Grid (2013). www.nationalgrideso.com/document/46916/download
41. Guidi, G., Fosso, O.: Investment cost of hvac cable reactive power compensation off-shore. In: 2012 IEEE International Energy Conference and Exhibition (ENERGYCON), pp. 299–304. IEEE, Piscataway (2012)
42. ABB.: PCS6000, full power converter, up to 12 MW. ABB (2019)
43. Li, R., Xu, L.: A unidirectional hybrid hvdc transmission system based on diode rectifier and full-bridge mmc. IEEE J. Emerging Sel. Top. Power Electron. (2020)
44. Walling, R., Ruddy, T.: Economic optimization of offshore windfarm substations and collection systems. Paper presented at fifth international

workshop on large scale integration of wind power and transmission networks for offshore windfarms, Glasgow, 7–8 April 2005
45. Dahmani, O., Bourguet, S., Machmoum, M., Guerin, P., Rhein, P., Josse, L.: Optimization and reliability evaluation of an offshore wind farm architecture. IEEE Trans. Sustain. Energy 8(2), 542–550 (2016)
46. Working Group B1. 10.: TB379: Update of Service Experience of HV Underground and Submarine Cable Systems. CIGRE, Paris (2009)
47. Frankén, B.: Reliability study: Analysis of electrical systems within offshore wind parks. Elforsk AB (2007)
48. MacIver, C.: A Reliability Evaluation of Offshore HVDC Transmission Network Options. University of Strathclyde, Glasgow (2015)
49. Fischer, K., Wenske, J.: Towards reliable power converters for wind turbines: Field-data based identification of weak points and cost drivers. In: Scientific Proceedings of EWEA. EWEA, Brussels (2015)
50. Working Group B4. 60.: TB713: Designing HVDC Grids for Optimal Reliability and Availability Performance. CIGRE, Paris (2017)
51. Negra, N.B., Holmstrom, O., Bak Jensen, B., Sorensen, P.: Aspects of relevance in offshore wind farm reliability assessment. IEEE Trans. Energy Convers. 22(1), 159–166 (2007)

How to cite this article: Timmers, V., Egea-Àlvarez, A., Gkountaras, A., Li, R., Xu, L.: All-DC offshore wind farms: When are they more cost-effective than AC designs? IET Renew. Power Gener. 1–13 (2022). https://doi.org/10.1049/rpg2.12550

APPENDICES A

A.1 | Cost equations

The median cost of the AC wind turbine is calculated using

$$C_{ACWT} = \underbrace{1.051}_{\text{inflation}} \cdot \left(\underbrace{1.374 \cdot \frac{P_T^{0.87}}{N_{WT}}}_{\text{wind turbine}} + \underbrace{0.363 \cdot P_{WT}^{1.06}}_{\text{foundation}} \right), \tag{A.1}$$

where C_{ACWT} is the cost of the AC wind turbines in M€$_{2021}$, P_T is the total active power of the wind farm, P_{WT} is the rated power of an individual wind turbine and N_{WT} is the number of wind turbines. An inflation factor of 1.051 is used to convert the costs to M€$_{2021}$.

The median cost of the AC collector cables is calculated using

$$C_{ACcab} = \underbrace{0.1437}_{\text{conversion}} \cdot \left(\underbrace{A_p + B_p \cdot \exp\left(\frac{C_p S_n}{100}\right)}_{\text{cable}} + \underbrace{2.4}_{\text{inst.}} \right), \tag{A.2}$$

where C_{ACcab} is the cable cost in M€$_{2021}$/km, A_p, B_p and C_p are constants dependent on the cable voltage, given in Table A.1, and S_n is the rated power of the cable in MVA. The original equation calculates the costs in SEK$_{2003}$, therefore a conversion factor of 0.1437 was used.

TABLE A.1 Cost parameters used in (A.2) for AC cables [12]

Voltage (kV)	A_p	B_p	C_p
33	0.411	0.596	4.1
66	0.688	0.625	2.05
132	1.971	0.209	1.66
220	3.181	0.11	1.16

TABLE A.2 Cost parameters used in (A.3) for DC cables [12]

Voltage (kV)	A_p	B_p
40	−0.314	0.0618
160	−0.100	0.0164
230	0.079	0.0120
300	0.286	0.0097

TABLE A.3 Cost parameters used in (A.4) for HV cables [37]

Parameter	HVAC	HVDC
A	$5.05 \cdot 10^{-6}$	$1.31 \cdot 10^{-7}$
B	$-1.32 \cdot 10^{-3}$	$1.47 \cdot 10^{-4}$
C	0.43	0.29
D	0.79	0.85

The median cost of the DC collector cables is calculated using

$$C_{DCcab} = \underbrace{0.1437}_{\text{conversion}} \left(\underbrace{A_p + B_p \cdot P_{cab}}_{\text{cable}} + \underbrace{2.4}_{\text{instal.}} \right), \tag{A.3}$$

where C_{DCcab} is the cost of the DC cables in M€$_{2021}$/km, P_{cab} is the rated power of the cable in MW, and A_p and B_p are parameters dependent on the voltage, given in Table A.2. For other voltages, the values of A_p and B_p are estimated using linear interpolation.

The median cost of HV cables can be approximated using the second-order equation

$$C_{HVcab} = \underbrace{1.452}_{\text{conversion}} \cdot \left(\underbrace{A \cdot P_{cab}^2 + B \cdot P_{cab} + C}_{\text{cable}} + \underbrace{D}_{\text{instal.}} \right), \tag{A.4}$$

where C_{HVcab} is the cost of the transmission cable in M€ $_{2021}$/km and P_{cab} is the rated power of the cable in MW. The parameters are given in Table A.3.

The median cost of the AC substation platform is calculated using

$$C_{ACpl} = \underbrace{1.0519}_{\text{inflation}} \cdot (0.0738 \cdot P_{WF} + 53.25), \tag{A.5}$$

where C_{ACpl} is the cost of the AC platform in M€ $_{2021}$ and P_{WF} is the rated power of the wind farm in MW.

The median cost of the DC platform is calculated using

$$C_{DCpl} = \underbrace{1.0519}_{\text{inflation}} \cdot (0.125 \cdot P_{WF} + 165), \tag{A.6}$$

where C_{DCpl} is the cost of the DC platform in M€ $_{2021}$ and P_{WF} is the rated power of the wind farm in MW.

The median cost of the high power converter is calculated based on [12], using the equation

$$C_{conv} = \underbrace{0.1437}_{\text{conversion}} \cdot P_{WF}, \tag{A.7}$$

where C_{conv} is the cost of either the AC/DC or DC/DC converter in M€ $_{2021}$ and P_{WF} is the rated power of the wind farm in MW. The original equation calculates the costs in SEK2003, therefore a conversion factor of 0.1437 was used.

The transformer cost is approximated using

$$C_{TR} = \underbrace{1.1495}_{\text{inflation}} \cdot \left(0.0427 \cdot (P_{TR})^{0.7513}\right), \tag{A.8}$$

where C_{TR} is the cost of the transformer in M€ $_{2021}$ and P_{TR} is the rated power of the transformer in MVA.

The switchgear cost can be approximated by the linear equation

$$C_{SG} = \underbrace{1.452}_{\text{conversion}} \cdot (0.0105 \cdot V_{SG} - 0.2007), \tag{A.9}$$

where C_{SG} is the cost of the switchgear in M€ $_{2021}$ and V_{SG} is the rated voltage of the switchgear in kV.

The cost of the shunt reactor is given by

$$C_{SR} = \underbrace{1.452}_{\text{conversion}} \cdot (0.0177 \cdot Q_{SR} + 0.96). \tag{A.10}$$

The additional platform cost due to shunt reactor weight is calculated using

$$C_{SRweight} = \underbrace{1.0844}_{\text{inflation}} \cdot \left(6.08 \cdot 10^{-4} \cdot Q_{SR}^{0.765}\right). \tag{A.11}$$